Materials Sciences and Applications, 2015, 6, 457-463
Published Online June 2015 in SciRes. http://www.scirp.org/journal/msa
http://dx.doi.org/10.4236/msa.2015.66049

Scientific Research Publishing

Structure Evolution in Austenitic Stainless Steels

—A State Variable Model Assessment

Paul S. Follansbee

Boyer School of Natural Sciences, Mathematics, and Computing, Saint Vincent College, Latrobe, USA
Email: paul.follansbee@stvincent.edu

Received 22 April 2015; accepted 26 May 2015; published 29 May 2015

Abstract

Strain hardening in austenitic stainless steels is modeled according to an internal state variable constitutive model. Derivation of model constants from published stress-strain curves over a range of test temperatures and strain rates is reviewed. Model constants for this material system published previously are revised to make them more consistent with model constants in other material systems.

Keywords

Constitutive Modeling, Internal State Variable, Austenitic Stainless Steel, Strain Hardening

1. Introduction

The constitutive behavior of annealed, austenitic stainless steels was recently analyzed according to an internal state variable model [1] [2]. In this model, which has been described in detail by Follansbee [2], the temperature and strain-rate dependent yield stress, σ, of annealed material (with a low initial dislocation density) is modeled as

$$\frac{\sigma}{\mu} = \frac{\sigma_a}{\mu} + s_i\left(\dot{\varepsilon}, T\right)\frac{\hat{\sigma}_i}{\mu_o} + s_N\left(\dot{\varepsilon}, T\right)\frac{\hat{\sigma}_N}{\mu_o} \tag{1}$$

where σ_a is an athermal stress (e.g., due to the strengthening contribution of grain boundaries), $\hat{\sigma}_i$ is an internal state variable characterizing the strengthening contribution of solute element additions, and $\hat{\sigma}_N$ is an internal state variable characterizing the strengthening contribution due to nitrogen, μ is the temperature-dependent shear modulus, μ_o is the shear modulus at 0 K, and s_i and s_N are functions (varying from zero to unity) that describe the

How to cite this paper: Follansbee, P.S. (2015) Structure Evolution in Austenitic Stainless Steels. *Materials Sciences and Applications*, **6**, 457-463. http://dx.doi.org/10.4236/msa.2015.66049

temperature (T) and strain rate $(\dot{\varepsilon})$ dependence of the two strength contributions. The explicit nitrogen-dependent term in Equation (1) evolved from analysis of two extensive data sets documenting the effect of the nitrogen content on the temperature-dependent yield stress in austenitic stainless steels [3] [4].

The addition of strain-hardening is modeled by adding another internal state variable to Equation (1):

$$\frac{\sigma}{\mu}=\frac{\sigma_a}{\mu}+s_i\left(\dot{\varepsilon},T\right)\frac{\hat{\sigma}_i}{\mu_o}+s_N\left(\dot{\varepsilon},T\right)\frac{\hat{\sigma}_N}{\mu_o}+s_\varepsilon\left(\dot{\varepsilon},T\right)\frac{\hat{\sigma}_\varepsilon\left(\varepsilon\right)}{\mu_o} \tag{2}$$

where $\hat{\sigma}_\varepsilon$ is the internal state variable characterizing interactions of mobile dislocations with stored (or immobile) dislocations and s_ε defines the temperature and strain-rate dependence of these interactions. The analysis of temperature and strain-rate dependent yield stress measurements in a variety of austenitic stainless steels led to the following definitions of s_i, s_N, and s_ε, where k is Boltzmann's constant and b is the Burgers vector:

$$s_i\left(\dot{\varepsilon},T\right)=\left\{1-\left[\frac{kT}{\mu b^3\left(0.20\right)}\ln\left(\frac{10^8\ \mathrm{s}^{-1}}{\dot{\varepsilon}}\right)\right]^{2/3}\right\}^2 \tag{3}$$

$$s_N\left(\dot{\varepsilon},T\right)=\left\{1-\left[\frac{kT}{\mu b^3\left(1.7\right)}\ln\left(\frac{\left(10^8\ \mathrm{s}^{-1}\right)}{\dot{\varepsilon}}\right)\right]^{2/3}\right\}^2 \tag{4}$$

$$s_\varepsilon\left(\dot{\varepsilon},T\right)=\left\{1-\left[\frac{kT}{\mu b^3\left(1.6\right)}\ln\left(\frac{10^7\ \mathrm{s}^{-1}}{\dot{\varepsilon}}\right)\right]^{1}\right\}^{3/2} \tag{5}$$

Consistent with an internal-state variable formulation, the strain-dependence of $\hat{\sigma}_\varepsilon$ is defined by the differential

$$\frac{\mathrm{d}\hat{\sigma}}{\mathrm{d}\varepsilon}=\theta_{\mathrm{II}}\left(1-\frac{\hat{\sigma}}{\hat{\sigma}_{es}\left(\dot{\varepsilon},T\right)}\right)^{\kappa} \tag{6}$$

where θ_{II} is the stage two hardening rate (e.g., of a single crystal), κ is a constant, and $\hat{\sigma}_{\varepsilon s}$ is the temperature and strain-rate dependence saturation threshold stress. When κ equals unity, Equation (3) becomes the Voce Law. According to Equation (6) the rate of strain hardening begins at θ_{II} and approaches zero as $\hat{\sigma}_\varepsilon$ approaches $\hat{\sigma}_{\varepsilon s}$. Finally, the temperature and strain rate dependence of $\hat{\sigma}_{\varepsilon s}$ is described using a dynamic recovery model [5]

$$\ln\hat{\sigma}_{\varepsilon s}=\ln\hat{\sigma}_{\varepsilon so}+\frac{kT}{\mu b^3 g_{\varepsilon so}}\ln\frac{\dot{\varepsilon}}{\dot{\varepsilon}_{\varepsilon so}} \tag{7}$$

where $\hat{\sigma}_{\varepsilon so}$ is the value of $\hat{\sigma}_{\varepsilon s}$ at 0 K, and $\dot{\varepsilon}_{\varepsilon so}$ and $g_{\varepsilon so}$ are constants. Values of the model constants in Equations (6) and (7) were listed in [1] and [2], but the analysis used to generate these constants was omitted. The purpose of this paper is to document this detail and to report updated values of these constants that are more in line with the constants for the other metals and alloys included in [2].

2. Evaluating the Evolution Equation

The temperature and strain-rate dependence of evolution (strain hardening) is evaluated by analyzing stress-strain curves measured at various temperatures and strain rates. Rewriting Equation (2),

$$\hat{\sigma}_\varepsilon\left(\varepsilon\right)=\frac{1}{s_\varepsilon\left(\dot{\varepsilon},T\right)}\left[\frac{\mu_o}{\mu}\left(\sigma\left(\varepsilon\right)-\sigma_a\right)-s_i\left(\dot{\varepsilon},T\right)\hat{\sigma}_i-s_N\left(\dot{\varepsilon},T\right)\hat{\sigma}_N\right] \tag{8}$$

A key premise of the internal-state variable model applied here is that evolution does not alter the parameters on the right-hand side of Equation (8)—except of course for $\sigma(\varepsilon)$. This premise was shown to be approximately valid by Follansbee and Kocks, through extensive measurements of the evolution of the internal state variable in pure copper [6]. In applying Equation (8) to stress-strain curves measured in an annealed austenitic stainless

steel, introduction of correct values of σ_a, $\hat{\sigma}_i$, and $\hat{\sigma}_N$ should give an initial value of $\hat{\sigma}_\varepsilon$ equal to zero, and the increase of $\hat{\sigma}_\varepsilon$ with strain should follow Equation (6). **Figure 1** shows the result of this analysis on a stress-strain curve reported by Albertini and Montagnani [7] in annealed 316 L stainless steel measured at 295 K and a strain rate of 0.004 s^{-1}. For this calculation, $\sigma_a = 50$ MPa, $\hat{\sigma}_i = 572$ MPa, and $\hat{\sigma}_N = 243$ MPa. As expected $\hat{\sigma}_\varepsilon$ starts close to zero and increases uniformly with strain. Application of Equation (8) to a more extensive data set is described in the next section.

3. Stress-Strain Measurements in AISI 304 and AISI 316 Stainless Steels

Table 1 lists the source of 18 measurements of stress-strain curves in AISI 304 and AISI 316 stainless steels (and variations of these alloys). The data set was selected because of the wide range of temperatures and strain rates investigated, which is necessary for evaluation of the constants in Equation (7). Included in **Table 1** are the grain sizes and the nitrogen contents (when specified). The nitrogen contents are listed because of the correlation of the state variable $\hat{\sigma}_N$ (as well as $\hat{\sigma}_i$) discussed in [1]. Each of these stress-strain curves was analyzed according to Equation (8) to derive the variation of $\hat{\sigma}_\varepsilon$ with strain. As in **Figure 1**, the values of σ_a and the two state variables were taken as $\sigma_a = 50$ MPa, $\hat{\sigma}_i = 572$ MPa, and $\hat{\sigma}_N = 243$ MPa. The slight variation in grain size could result in σ_a values slightly greater than (for a smaller grain size) or less than (for a larger grain size) the assumed 50 MPa, but this would be a small effect. Similarly, the variation in nitrogen content could result in $\hat{\sigma}_i$ and $\hat{\sigma}_N$ values that differ from the assumed values of 572 MPa and 243 MPa, respectively. The net result of using the assumed values of these parameters on the predicted $\hat{\sigma}_\varepsilon$ values is that in softer materials (e.g., AISI 304 versus AISI 316, or AISI 316 LN versus AISI 316), the $\hat{\sigma}_\varepsilon$ values would start off negative at zero strain. This can be easily accounted for by adding an "offset" stress so that the $\hat{\sigma}_\varepsilon$ values start at zero. The value of the offset used in the calculations is listed in **Table 1**. Indeed, negative offsets are generally observed in the softer materials, but there some outliers. For instance, there is no reason for the offset stress to differ for tests at different temperatures on the same material. That this is found in a few cases demonstrates the level of experimental scatter in the measurements and analysis.

The next step of the analysis is to fit Equation (6) to the $\hat{\sigma}_\varepsilon$ versus ε curves. In [1] and [2] κ was selected as 3.4, which led to $\hat{\sigma}_{\varepsilon so} = 4000$ MPa, $\dot{\varepsilon}_{\varepsilon so} = 10^5$ s^{-1}, and $g_{\varepsilon so} = 0.25$. While these model parameters enabled close fits with the measurements, they differed from the model parameters published in [2] for a large collection of FCC, BCC, and HCP metals and alloys. In particular the κ—value for these other systems was either $\kappa = 1$ or $\kappa = 2$. Secondly, the $\hat{\sigma}_{\varepsilon so}$ value (4000 MPa) was much higher than estimated in all of the other materials. In all of the other systems analyzed, $0.009 < \hat{\sigma}_{\varepsilon so}/\mu_o < 0.035$. For the austenitic stainless steels, $\hat{\sigma}_{\varepsilon so}/\mu_o = 0.056$. Finally, the typical value of $\dot{\varepsilon}_{\varepsilon so}$ is 10^7 s^{-1}. Inspection of Equation (6) indicates that κ and $\hat{\sigma}_{\varepsilon so}$ are not completely independent; a high value of κ along with a high value of $\hat{\sigma}_{\varepsilon so}$ yields an almost identical stress strain curve over the strain range of interest as a low value of κ along with a low value of $\hat{\sigma}_{\varepsilon so}$. **Figure 2** shows an example fit of a $\hat{\sigma}_\varepsilon$ versus ε curve for the data set given in **Figure 1**. The two dashed curves are the model fits. The short-dashed curve is for the model parameters listed above. The long-dashed curve uses κ = 2,

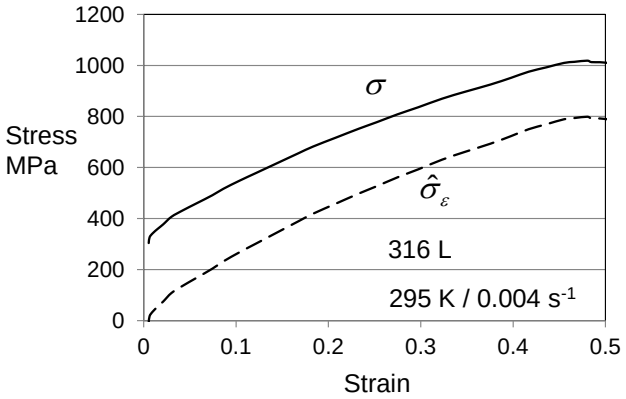

Figure 1. Analysis of the Albertini and Montagnani stress-strain curve at 295 K and a strain rate of 0.004 s^{-1} according to Equation (8) to give $\hat{\sigma}_\varepsilon$ versus strain.

Table 1. Stress-strain measurements in annealed AISI 316 and AISI 304 stainless steels (and variations of these alloys) analyzed in this study.

Source (Primary Author)	Material Characteristics and Testing Conditions					Analysis Results		
	Material	Grain Size	Strain Rate (s^{-1})	Temp (K)[a]	Nitrogen %	Offset (MPa)	$\hat{\sigma}_{\varepsilon s}$ (MPa)	θ_{II} (MPa)
Steichen [8]	304	ASTM 5 (63 μm)	3×10^{-5}	811	0.052	+30	2200	2800
			100	811 (829)		–60	1200	3250
Albertini [7]	316L	"Virgin" condition	0.0035	823	– –	+50	2000	2900
			44	295 (381)		+60	1600	3400
Semiatin [9]	304L	ASTM 7.5 (27 μm)	0.004	295	0.038	0	1850	3000
			0.01	294		0	2300	2900
			0.0035	673		0	950	3000
Conway [10]	316	– –[b]	0.004	294	0.05	0	2200	2885
			0.004	703		0	2300	3000
Byun [11]	316	– –[c]	0.001	294	0.031	0	2100	2900
			0.001	437		0	1750	2900
Dai [12]	316 LN	– –[c]	0.001	294	0.067	–100	1800	2850
			0.001	523		–50	1500	2900
			0.001	623		0	2400	2850
Stout [13]	304L	40 μm	0.0002	295	0.082	–25	2200	3000
			0.02	295		–25	2300	3100
			100	295 (371)		–100	2200	3200
Antoun [14]	304	– –	0.0001	344	– –	–80	1550	2850

[a]The final temperatures for tests under adiabatic conditions are listed in parentheses; [b]The material received a "stress relief anneal"; these treatments are well above the recrystallization temperature of 850˚C and would yield a grain size of 30 μm to 60 μm, depending on the heat treatment time [15]; [c]The material was reportedly heat treated at 1050˚C for 30 minutes; this is a common solution anneal condition, also well above the recrystallization temperature of 850˚C, that would yield a grain size of 40 μm to 60 μm [15].

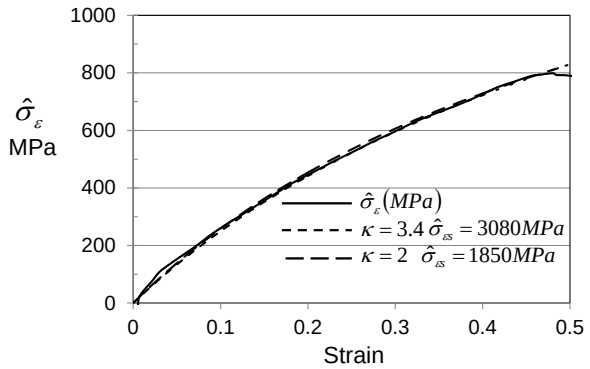

Figure 2. Fit of Equation (6) to the deduced values of $\hat{\sigma}_\varepsilon$ versus strain curve deduced for the Albertini and Montagnani stress-strain curve at 295 K and a strain rate of 0.004 s^{-1}. Two sets of model parameters are used to demonstrate the interplay between *k* and $\hat{\sigma}_\varepsilon$.

$\hat{\sigma}_{\varepsilon so} = 2600$ MPa, $\dot{\varepsilon}_{\varepsilon so} = 10^7\ s^{-1}$, and $g_{\varepsilon so} = 0.258$[1]. It is evident that the two model curves are almost coincident.

Each of the measurements listed in **Table 1** was analyzed with $\kappa = 2$ as described above. Model parameters ($\hat{\sigma}_{\varepsilon s}$ and θ_{II}) that yielded a good match of Equation 6 with the measurements are listed in the last two columns of **Table 1**. Fits of $\hat{\sigma}_\varepsilon$ versus strain for two of these measurements are shown in **Figure 3**. The solid curves are

[1]Only a $\kappa = 2$ is selected; the remaining parameters arise from the fit to the full data set listed in **Table 1** as described below. Agreement with the data, although, is not as good with $\kappa = 1$.

the deduced values of $\hat{\sigma}_{\varepsilon}$ versus strain; the dashed curves are the model predictions according to Equation 6 with the model parameters listed in **Table 1**. The lower curves are from the Antoun measurements in 304 SS at 344 K and a strain rate of 0.001 s^{-1} [14]. The curves at the higher stress levels are for the measurement by Stout and Follansbee in AISI 304L at 295 K and a strain rate of 100 s^{-1} [13].

The parameters in the last column of **Table 1** suggest a slight strain-rate dependence of θ_{II}. While the extensive measurements by Follansbee and Kocks in copper [6] indicated this strain-rate dependence, one would not conclude this with the limited data set in the stainless steels presented here. The indicated strain-rate dependence is assumed based on the earlier measurements, and the assumed correlation is

$$\theta_{II} = 3120\ \text{MPa} + 32\ \text{MPa}\ln\left(\dot{\varepsilon}\right) \tag{9}$$

where the strain rate $\dot{\varepsilon}$ has the units s^{-1}. Equation (9) is very close to the result published earlier [1] [2], where the constant was 3010 MPa and the multiplier of the logarithmic term was 23 MPa.

The dependence of $\hat{\sigma}_{\varepsilon s}$ on temperature[2] and strain rate is evaluated using Equation (7), shown in **Figure 4**. The data points plotted as open triangles fall roughly on a line when $\hat{\sigma}_{\varepsilon so}$ in Equation (7) is set at 2600 MPa and $\dot{\varepsilon}_{\varepsilon so}$ from Equation (7) is set at 10^7 s^{-1}. Note that the dashed line passes through the origin, which is consistent with Equation (7). From the slope of the line, the value of $g_{\varepsilon so}$ is found to be 0.258.

The four open squares in **Figure 4** that fall well off the line are for the Albertini and Montagnani data set at 823 K [7] , the Steichen data set at 811 K and a strain rate of 3×10^{-5} s^{-1} [8] , the Conway et al data set at 703 K [10], and the Dai et al data set at 623 K [12]. It was proposed in [2] that dynamic strain aging becomes active at these high temperatures, which leads to behavior that deviates strongly from that described by Equation (7). A method to include the higher stresses during dynamic strain aging into the constitutive model was introduced in [2].

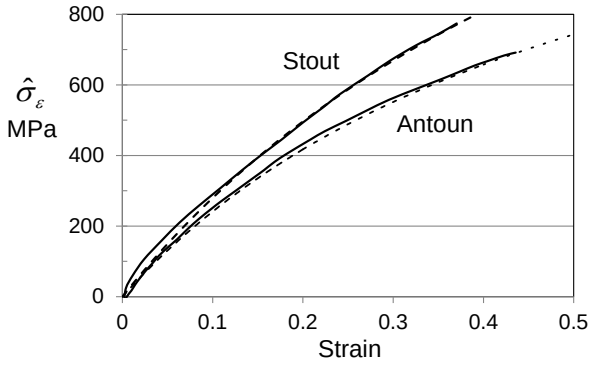

Figure 3. Fit of Equation (6) to the Stout and Follansbee stress-strain curve in 304L SS at 295 K and a strain rate of 100 s^{-1} and the Antoun stress-strain curve in 304 SS at 344 K and a strain rate of 0.001 s^{-1}.

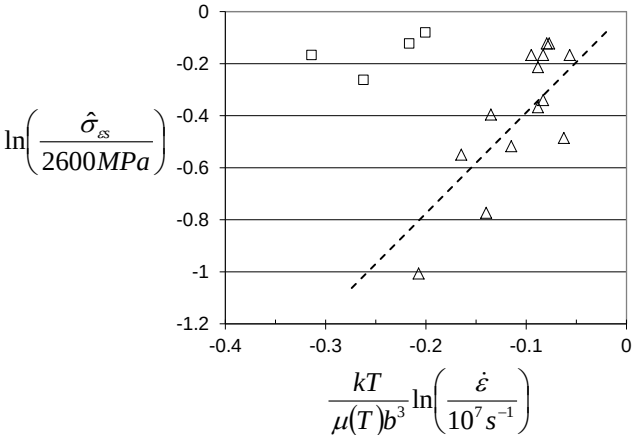

Figure 4. Saturation threshold stress $(\hat{\sigma}_{\varepsilon s})$ versus temperature and strain rate according to Equation (7).

[2]For the three adiabatic tests, the final rather than the initial temperature is plotted in **Figure 4**.

4. Summary

Analysis of stress-strain curves reported for annealed austenitic stainless steels has given further evidence of the application of the internal state variable constitutive formulism developed by the author and coworkers. Of particular interest here was the derivation of model parameters describing strain-hardening. A set of model parameters for this alloy system was given in previous publications [1] [2], but the derivation of these parameters was not presented in these earlier publications.

The reanalysis of the literature stress-strain curves presented here demonstrated that the model parameters in Equations (6) and (7) are somewhat co-dependent. In particular, a high value of κ along with a high value of $\hat{\sigma}_{\varepsilon so}$ can give almost identical agreement with a specific $\hat{\sigma}_{\varepsilon}$ versus ε data set as a low value of κ along with a low value of $\hat{\sigma}_{\varepsilon so}$ over the strain range of interest ($\varepsilon < 1$). The proposed value of $\kappa = 2$ for the austenitic stainless steels is more in line with model parameters proposed for a wide variety of material systems. The interplay between κ and $\hat{\sigma}_{\varepsilon so}$ reinforces a conclusion reached in [2] (see Chapter 13) that the empirically based hardening (or structure evolution) model (particularly with $\kappa \neq 1$) lacks a sound mechanistic foundation. Future work on this element of the model would enhance the internal state variable model formulation.

Acknowledgements

The author appreciates the support of Saint Vincent College in the writing of [2] and the compilation of this manuscript.

References

[1] Follansbee, P.S. (2012) An Internal State Variable Constitutive Model for Deformation of Austenitic Stainless Steels. *Journal of Engineering Materials and Technology*, **134**, 41007-1-41007-10. http://dx.doi.org/10.1115/1.4006822

[2] Follansbee, P.S. (2014) Fundamentals of Strength—Principles, Experiment, and Application of an Internal State Variable, Constitutive Formulation. The Minerals, Metals, & Materials Society, John Wiley & Sons, Hoboken.

[3] Norström, L.-Å. (1977) The Influence of Nitrogen and Grain Size on Yield Strength in Type AISI 316L Austenitic, Stainless Steel. *Metal Science*, **11**, 208-212. http://dx.doi.org/10.1179/msc.1977.11.6.208

[4] Brynes, M.L.G., Grujicic, M. and Owen, W.S. (1987) Nitrogen Strengthening of a Stable Austenitic Stainless Steel. *Acta Metallurgia*, **37**, 1853-1862. http://dx.doi.org/10.1016/0001-6160(87)90131-3

[5] Kocks, U.F. (1976) Laws for Work-Hardening and Low-Temperature Creep. *ASME Journal of Engineering Materials and Technology*, **98**, 76-85. http://dx.doi.org/10.1115/1.3443340

[6] Follansbee, P.S. and Kocks, U.F. (1988) A Constitutive Description of the Deformation of Copper Based on the Use of the Mechanical Threshold Stress as an Internal State Variable. *Acta Metallurgica*, **36**, 81-93. http://dx.doi.org/10.1016/0001-6160(88)90030-2

[7] Albertini, C. and Montagnani, M. (1980) Dynamic Uniaxial and Biaxial Stress-Strain Relationships for Austenitic Stainless Steels. *Nuclear Engineering and Design*, **57**, 107-123. http://dx.doi.org/10.1016/0029-5493(80)90226-5

[8] Steichen, J.M. (1971) High Strain Rate Mechanical Properties of Types 304 Stainless Steel and Nickel 200 (RM-14). Hanford Engineering Development Laboratory, HEDL-TME-71-145, Richland, WA.

[9] Semiatin, S.L. and Holbrook, J.H. (1982) Isothermal Plastic Flow Behavior of Annealed 304L Stainless Steel. Final Technical Report to Sandia National Laboratories, Contract Number SN4156-PO92-9342, Battelle Columbus Laboratories.

[10] Conway, J.B., Stentz, R.H. and Berling, J.T. (1974) Fatigue, Tensile, and Relaxation Behavior of Stainless Steels. Report commissioned by the US Atomic Energy Commission, Division of Reactor Research and Development, NTIS, TID26135.

[11] Byun, T.S., Hashimoto, N. and Farrell, K. (2004) Temperature Dependence of Strain Hardening and Plastic Instability Behaviors in Austenitic Stainless Steels. *Acta Materialia*, **52**, 3889-3899. http://dx.doi.org/10.1016/j.actamat.2004.05.003

[12] Dai, Y., Egeland, G.W. and Long, B. (2008) Tensile Properties of ECX316LN Irradiated in SINQ to 20 dpa. *Journal of Nuclear Materials*, **377**, 109-114. http://dx.doi.org/10.1016/j.jnucmat.2008.02.035

[13] Stout, M.G. and Follansbee, P.S. (1986) Strain Rate Sensitivity, Strain Hardening, and Yield Behavior of 304L Stainless Steel. *Journal of Engineering Materials and Technology*, **108**, 344-353. http://dx.doi.org/10.1115/1.3225893

[14] Antoun, B.R. (2004) Temperature Effects on the Mechanical Properties of Annealed and HERF 304L Stainless Steel. Sandia National Laboratories, Sandia Report, SAND2004-3090.

[15] Schino, A.D., Abbruzzese, G. and Kenny, J.M. (2003) Recrystallization and Grain Growth in Austenitic Stainless Steels: A Statistical Approach. *Journal of Materials Science &Technology*, **19**, 119-121.